Simple QED- and QCD-like Models at Finite Density

Jan M. Pawlowski,[1,2] Ion-Olimpiu Stamatescu,[1,3] and Christian Zielinski[1,4]

[1] *Institut für Theoretische Physik, Universität Heidelberg, Philosophenweg 16, 69120 Heidelberg, Germany*
[2] *ExtreMe Matter Institute EMMI, GSI, Planckstraße 1, D-64291 Darmstadt, Germany*
[3] *FEST, Schmeilweg 5, 69118 Heidelberg, Germany*
[4] *Division of Mathematical Sciences, Nanyang Technological University, Singapore 637371*

(Dated: February 26, 2014)

In this paper we discuss one-dimensional models reproducing some features of quantum electrodynamics and quantum chromodynamics at non-zero density and temperature. Since a severe sign problem makes a numerical treatment of QED and QCD at high density difficult, such models help to explore various effects peculiar to the full theory. For these models we evaluate the respective partition functions and discuss several observables as well as the Silver Blaze phenomenon. Despite the simplicity of the underlying models, we find many interesting physical properties.

PACS numbers: 11.15.Ha, 12.38.Gc, 12.38.-td
Keywords: Sign problem, finite density, quantum chromodynamics, quantum electrodynamics

arXiv:1402.6042v1 [hep-lat] 25 Feb 2014

I. Introduction

One of the open challenges of lattice gauge theory is the *ab initio* treatment of full quantum chromodynamics (QCD) at finite density and low temperature. The fermion determinant is rendered complex and rapidly oscillating after the introduction of a finite chemical potential μ. The same holds for a wide spectrum of theories at non-zero density. The resulting near-cancellations makes an evaluation of expectation values extremely challenging. Several methods for meeting the sign problem have been advanced, but are either limited in their applicability or are about to be tested for QCD, see e.g. Refs. [1–11].

In the past, studies of models of QCD have been proved insightful [12–17], including in the special case of HQCD [15, 18, 19], i.e. QCD with heavy quarks and large chemical potentials. Some simple models permitting analytical calculations can also be used to test new simulation algorithms. Examples can be found in Refs. [15–17, 20].

In this paper, we construct and study models that exhibit properties of quantum electrodynamics (QED) and quantum chromodynamics at non-zero μ and finite T. These models are formulated on a one-dimensional lattice using staggered fermions [21–24]. In comparison to the corresponding full theories, these models have severe simplifications. In particular, as it is not possible to define a plaquette variable in one dimension, we only have a global gauge symmetry instead of a local one. Nevertheless, the simple models exhibit interesting phenomena that are peculiar to more elaborated models and theories.

The resulting partition function can be fully integrated for a U(1) gauge group. In the case of SU(3) we are left with an integral expression, whose sign problem is manageable and which can be numerically evaluated. We discuss some observables and investigate the Silver Blaze phenomenon [25] in these models. A theory exhibits Silver Blaze behavior, if in the zero-temperature limit $T \to 0$ observables become independent of the chemical potential for $\mu \leq \mu_{\rm crit}$, where $\mu_{\rm crit}$ is some critical onset value of the chemical potential. In realistic models $\mu_{\rm crit} = m_q^{\rm phys}$ corresponds to the physical fermion mass, or, more generally, the mass of the lowest excitation with non-vanishing quark number.

We note that our models generalize the one-link models presented in Ref. [15]. While it is not possible to formulate the Yang-Mills action in one dimension, the present models mimic some properties of Yang-Mills theories via a suitably chosen purely bosonic part in the action. This, in addition to the particular form of the fermion matrix and the integration over conjugacy classes, results in the QCD-like model of Sec. III which differs from Refs. [13, 14, 16, 17].

We organize the paper as follows: first we introduce a QED-like model in Sec. II. We derive a closed expression for the partition function and discuss the dependence of some observables on chemical potential and temperature. In Sec. III we deal with the case of QCD and derive an integral expression, which can be numerically evaluated. In Sec. IV we discuss and summarize our findings.

II. A soluble, QED-like model at non-zero density

For the construction of a QED-like model we formulate an abelian U(1) lattice gauge theory on a finite one-dimensional lattice with staggered fermions and couple them to a chemical potential, following a similar ansatz as employed in previous works.

1. Partition function

The action we employ mimics the usual compact lattice QED in one dimension. The lattice is assumed to have a lattice spacing of a and an extension of N sites, where N is assumed to be even. We set $a = 1$, i.e., we measure all dimensionful quantities in appropriate powers of a. We consider a single staggered fermion field and couple it to a chemical potential μ. The temperature is identified with the inverse of the lattice extension $T = N^{-1}$. The

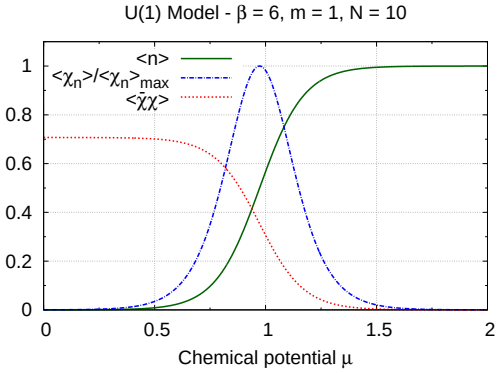

(a) Density, condensate and normalized susceptibility.

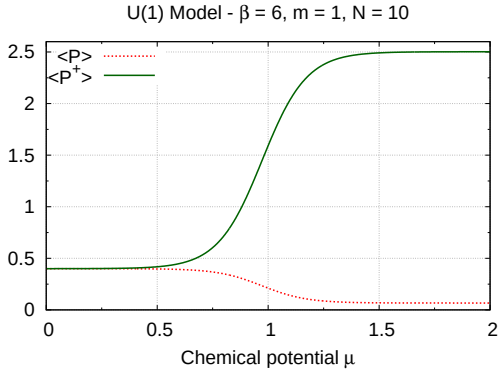

(b) Polyakov loop and conjugate Polyakov loop.

Figure 1: Observables in the U(1) model.

action $S = S_\mathrm{f} + S_\mathrm{g}$ consists of the fermionic part

$$S_\mathrm{f} = \sum_{t,\tau=1}^{N} \overline{\chi}\,(t)\, K\,(t,\tau)\, \chi\,(\tau)\ , \tag{1}$$

and the pure bosonic part

$$S_\mathrm{g} = \beta \sum_{t=1}^{N} \left[1 - \frac{1}{2}\left(U_t + U_t^\dagger\right)\right] . \tag{2}$$

Here $\overline{\chi}$ and χ denote the staggered fermion field, $K\,(t,\tau)$ the fermion matrix, $\beta = 1/e^2$ the inverse coupling constant and $U_t \in \mathrm{U}(1)$ the link variables. The fermion matrix reads

$$K\,(t,\tau) = \frac{1}{2}\left(U_t e^{\mu}\delta_{t+1,\tau} - U_\tau^\dagger e^{-\mu}\delta_{t-1,\tau}\right) + m\delta_{t\tau}\ , \tag{3}$$

with m denoting the mass of the fermion. The introduction of the chemical potential μ follows the prescription by Hasenfratz and Karsch [26]. Furthermore we impose an antiperiodic boundary condition for the fermionic field. After integrating out the fermionic degrees of freedom, the partition function reads

$$Z = \int \prod_{t=1}^{N} \mathrm{d}U_t\ \det K\, e^{-S_\mathrm{G}}\ . \tag{4}$$

In this case the fermion determinant can be evaluated analytically using identity (1) derived in Ref. [27]. We find

$$2^N \det K = e^{N\mu} \prod_t U_t + e^{-N\mu} \prod_\tau U_\tau^\dagger + 2\rho_+\ , \tag{5}$$

where we have introduced

$$\rho_\pm = \lambda_+ \pm \lambda_-\ , \qquad \lambda_\pm = \frac{1}{2}\left(m \pm \sqrt{1+m^2}\right)^N\ . \tag{6}$$

Note that Eq. (5), like full QED, satisfies the identity

$$\det K\,(\mu) = \left[\det K\,(-\mu^\star)\right]^\star\ , \tag{7}$$

which shows that in general the fermion determinant is complex for $\mu > 0$. We parametrize the link variables as $U_t = \exp\left(\mathrm{i}\phi_t\right)$ in terms of algebra-valued fields $\phi_t \in [0, 2\pi)$. The corresponding U(1)-Haar measure reads

$$\int \mathrm{d}U_t = \int_0^{2\pi} \frac{\mathrm{d}\phi_t}{2\pi}\ . \tag{8}$$

With this parametrization, the action in Eq. (2) takes the form

$$S_\mathrm{g} = \beta \sum_{t=1}^{N} \left(1 - \cos\phi_t\right)\ . \tag{9}$$

This allows us to integrate the partition function given in Eq. (4) by using the expression we derived for the fermion determinant in Eq. (5), to find

$$Z = \frac{e^{-\beta N}}{2^{N-1}}\left[\rho_+ I_0^N\,(\beta) + \cosh\left(N\mu\right) I_1^N\,(\beta)\right]\ . \tag{10}$$

Here I_n denotes the modified Bessel functions of the first kind.

2. *Observables*

Given the final expression for the partition function in Eq. (10), we can easily calculate any observable of interest. The density follows from $\langle n\rangle = N^{-1}\partial_\mu \log Z$, the respective susceptibility is defined as $\langle\chi_n\rangle = \partial_\mu\langle n\rangle$ and the fermion condensate is given by $\langle\overline{\chi}\chi\rangle = N^{-1}\partial_m \log Z$. These definitions leads us to the density,

$$\langle n\rangle = \frac{\sinh\left(N\mu\right) I_1^N\,(\beta)}{\rho_+ I_0^N\,(\beta) + \cosh\left(N\mu\right) I_1^N\,(\beta)}\ , \tag{11}$$

and the fermion condensate,

$$\langle\overline{\chi}\chi\rangle = \frac{\left(1+m^2\right)^{-1/2}\rho_- I_0^N(\beta)}{\rho_+ I_0^N(\beta) + \cosh(N\mu)\, I_1^N(\beta)}\,. \tag{12}$$

By directly evaluating the respective path integral expression, we find for the Polyakov loop $\mathcal{P} = \prod_t U_t$ the expectation value

$$\langle\mathcal{P}\rangle = \frac{e^{-\beta N}}{2^N Z}\left[2\rho_+ I_1^N(\beta) + e^{N\mu} I_2^N(\beta) + e^{-N\mu} I_0^N(\beta)\right]. \tag{13}$$

The conjugate Polyakov loop $\mathcal{P}^\dagger = \prod_t U_t^\dagger$ follows from a simple symmetry argument as $\langle\mathcal{P}^\dagger\rangle_\mu = \langle\mathcal{P}\rangle_{-\mu}$, cf. Ref. [16].

In Fig. 1 we show the density given by Eq. (11), the fermion condensate by Eq. (12) and the Polyakov loop by Eq. (13) as functions of the chemical potential μ. We see that already for $T = 1/N = 1/10$ the observables only show a weak dependence on the chemical potential below some critical value μ_{crit}. This shows how the Silver Blaze behavior [25] becomes apparent in this model, which strictly only holds in the limit $T \to 0$.

Close to $\mu \approx \mu_{\text{crit}}$ we also observe a fast increase or decrease of the observables before reaching the saturation regime. Note that the limits $\mu \to \infty$ and $\beta \to 0$ do not commute. Density and condensate behave as one would expect. The expectation values of $\mathcal{P}$ and $\mathcal{P}^\dagger$ approach

$$\langle\mathcal{P}\rangle \to \left[\frac{I_2(\beta)}{I_1(\beta)}\right]^N, \qquad \langle\mathcal{P}^\dagger\rangle \to \left[\frac{I_0(\beta)}{I_1(\beta)}\right]^N, \tag{14}$$

for $\mu \to \infty$. The Polyakov loop quickly drops to a typically small value with increasing μ while the conjugate Polyakov loop grows to a saturation value which diverges when $\beta \to 0$.

III. A QCD-like model at non-zero density

Now we extend the previous model to the non-abelian gauge group SU(3). By restricting the integration over the full gauge group to the respective conjugacy classes of SU(3), we will be able to reduce the partition function to an integral expression with a manageable sign problem.

3. Partition function

Our starting point is again the path integral expression for the partition function in Eq. (4), where now the pure bosonic part of the action reads

$$S_{\text{g}} = \beta\sum_{t=1}^{N}\left[1 - \frac{1}{6}\,\text{Tr}_{\text{c}}\left(U_t + U_t^\dagger\right)\right]. \tag{15}$$

Here $\beta = 6/g^2$ denotes the inverse coupling, $U_t \in \text{SU}(3)$ the link variables and Tr_{c} a trace in color space. Furthermore we replace the fermion matrix by

$$K(t,\tau) = \frac{1}{2}\left(\sigma_+ U_t e^{\mu}\delta_{t+1,\tau} - \sigma_- U_\tau^\dagger e^{-\mu}\delta_{t-1,\tau}\right) + m\delta_{t\tau}\,, \tag{16}$$

with $\sigma_\pm = \frac{1}{2}(\mathbb{1} \pm \sigma_3)$ and the third Pauli matrix $\sigma_3 = \text{diag}(1,-1)$. In the loop expansion this suppresses back steps, thus simulating a special feature of Wilson fermions. This choice results in a factorization of the fermion determinant of the form

$$\det K = \det_{\text{t,c}}\mathcal{K}_f \cdot \det_{\text{t,c}}\mathcal{K}_b\,, \tag{17}$$

where we introduced

$$\begin{aligned}\det_{\text{t,c}}\mathcal{K}_f &= \det_{\text{t,c}}\left(m\delta_{t\tau} + \frac{1}{2}U_t e^{\mu}\delta_{t+1,\tau}\right),\\ \det_{\text{t,c}}\mathcal{K}_b &= \det_{\text{t,c}}\left(m\delta_{t\tau} - \frac{1}{2}U_\tau^\dagger e^{-\mu}\delta_{t-1,\tau}\right).\end{aligned} \tag{18}$$

Here $U_{N+1} = -U_1$ and $\det_{\text{t,c}}$ refers to a determinant in position and color space.

In the following we restrict ourselves to observables which only depend on the conjugacy class of the link variables. We then replace the integration over the full gauge group SU(3) with an integration over these conjugacy classes. This idea and the factorization given in Eq. (17) were also previously exploited in a one link model in Ref. [15]. We thus parametrize the links by

$$U_t = \text{diag}\left(e^{\text{i}\phi_t}, e^{\text{i}\vartheta_t}, e^{-\text{i}(\phi_t+\vartheta_t)}\right), \tag{19}$$

with $\phi_t, \vartheta_t \in (-\pi, \pi]$. Ignoring a normalization constant, the Haar measure is given by $\text{d}U_t \propto J(\phi_t,\vartheta_t)\,\text{d}\phi_t\,\text{d}\vartheta_t$ with

$$\begin{aligned}J(\phi_t,\vartheta_t) = \sin^2\left(\frac{\phi_t-\vartheta_t}{2}\right)&\\ \times \sin^2\left(\frac{\phi_t+2\vartheta_t}{2}\right)\sin^2\left(\frac{2\phi_t+\vartheta_t}{2}\right)&,\end{aligned} \tag{20}$$

while the bosonic part of the action takes the form

$$S_{\text{g}} = \beta\sum_{t=1}^{N}\left[1 - \frac{1}{3}\left(\cos\phi_t + \cos\vartheta_t + \cos(\phi_t+\vartheta_t)\right)\right]. \tag{21}$$

The determinant in position space has a simple structure and can be analytically evaluated, e.g. directly or by resummation of the loop expansion for Eq. (16). For the remaining determinant in color space we use the identity

$$\det_{\text{c}}(\mathbb{1} + \alpha U_t) = 1 + \alpha\,\text{Tr}_{\text{c}}\,U_t + \alpha^2\,\text{Tr}_{\text{c}}\,U_t^{-1} + \alpha^3\,, \tag{22}$$

valid for all $A \in \text{SL}_3(\mathbb{C})$, see Ref. [15]. We can express the result in terms of the (conjugate) Polyakov loop

$$\begin{aligned}\det_{\text{t,c}}\mathcal{K}_f &= m^{3N}\det_{\text{c}}\left(\mathbb{1} + \xi_f\prod_t U_t\right)\\ &= m^{3N}\left(1 + \xi_f\mathcal{P} + \xi_f^2\mathcal{P}^\dagger + \xi_f^3\right),\end{aligned} \tag{23}$$

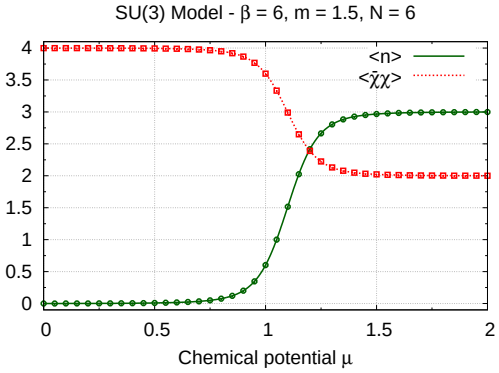

(a) Density and condensate.

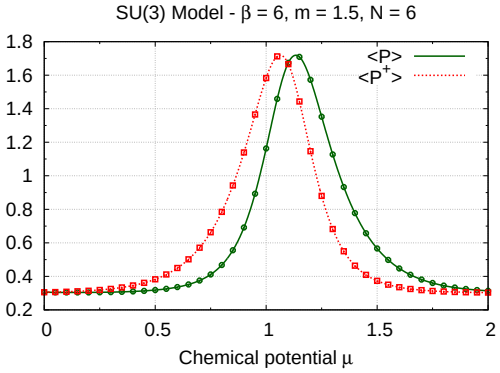

(b) Polyakov loop and conjugate Polyakov loop.

Figure 2: Observables in the SU(3) model.

with $\xi_f = [\kappa \exp(\mu)]^N$ and hopping parameter $\kappa = 1/(2m)$. The Polyakov loop $\mathcal{P}$ and conjugate Polyakov loop $\mathcal{P}^\dagger$ are defined by

$$\mathcal{P} = \mathrm{Tr_c} \prod_{t=1}^{N} U_t \,, \qquad \mathcal{P}^\dagger = \mathrm{Tr_c} \prod_{t=1}^{N} U_t^\dagger \,. \tag{24}$$

Analogously, we find

$$\det\nolimits_{\mathrm{t,c}} \mathcal{K}_b = m^{3N} \left(1 + \xi_b \mathcal{P}^\dagger + \xi_b^2 \mathcal{P} + \xi_b^3\right) \,, \tag{25}$$

with $\xi_b = [\kappa \exp(-\mu)]^N$. We observe that, as in the QED-like model, the fermion determinant in Eq. (17) satisfies the relation in Eq. (7).

Putting all pieces together, we find that the partition function of the model reads

$$Z = m^{6N} \int_{-\pi}^{\pi} \left[\prod_t \mathrm{d}\phi_t \, \mathrm{d}\vartheta_t \, J(\phi_t, \vartheta_t)\right] \left(1 + \xi_f \mathcal{P} + \xi_f^2 \mathcal{P}^\dagger + \xi_f^3\right) \left(1 + \xi_b \mathcal{P}^\dagger + \xi_b^2 \mathcal{P} + \xi_b^3\right) e^{-S_\mathrm{g}} \,, \tag{26}$$

where an irrelevant numerical normalization constant has been dropped. The measure term $J(\phi_t, \vartheta_t)$ was given in Eq. (20), S_g was introduced in Eq. (21).

4. *Observables*

Considering Eq. (26) as a model for QCD with the partition function Z, we can derive integral expressions for the density, the susceptibility and the fermion condensate by taking corresponding derivatives of $\log Z$. For the Polyakov loop and the conjugate Polyakov loop we insert a $\frac{1}{Z}\mathcal{P}$ or a $\frac{1}{Z}\mathcal{P}^\dagger$ term in Eq. (26).

The resulting integral expressions are numerically evaluated. Typical examples of these observables can be found in Fig. 2. The density and the condensate show similar qualitative behavior to the corresponding observables in the U(1) model, where we now find $\langle n \rangle \to 3$ for $\mu \to \infty$.

The Polyakov loop and conjugate Polyakov loop show some non-trivial behavior. Close to the critical onset μ_crit, we find peaks in $\langle \mathcal{P} \rangle$ and $\langle \mathcal{P}^\dagger \rangle$ with the peak in the conjugate Polyakov loop appearing at smaller μ. Similar behavior was previously observed in a simulation of a gauge theory with exceptional group G_2 [28], a strong coupling limit in HQCD [20], a three-dimensional effective theory of nuclear matter [19] and in recent studies of one-dimensional QCD [16, 17]. The drop of the Polyakov loop at high density is easily understood as an effect of saturation, while the displacement of the peaks has a dynamical basis, see, e.g. Ref. [20].

IV. Conclusions

In this paper we have constructed one-dimensional lattice models resembling QED and QCD to investigate the finite density and finite temperature regime. Despite the

drastic simplifications in these models, they capture some essential physical properties expected from the full theory and show an interesting behavior of the observables. We found that they—like their four-dimensional continuous counterparts—show the Silver Blaze property in the zero temperature limit $N \to \infty$. The μ-dependence of the SU(3) (conjugate) Polyakov loop $\mathcal{P}$ ($\mathcal{P}^\dagger$) shows the peculiar μ-dependence also found in other approximations of QCD. The models presented here can also serve as a starting point for the construction of more elaborated models.

V. Acknowledgments

This work is supported by the Helmholtz Alliance HA216/EMMI and by ERC-AdG-290623. JMP thanks the Yukawa Institute for Theoretical Physics, Kyoto University, where this work was completed during the YITP-T-13-05 on 'New Frontiers in QCD'. I.-O.S. thanks DFG for support.

[1] P. de Forcrand, PoS **LAT2009**, 010 (2009), arXiv:1005.0539 [hep-lat].
[2] M. Lombardo, Mod.Phys.Lett. **A22**, 457 (2007), arXiv:hep-lat/0509180 [hep-lat].
[3] G. Aarts, PoS **LAT2009**, 024 (2009), arXiv:0910.3772 [hep-lat].
[4] G. Aarts, L. Bongiovanni, E. Seiler, D. Sexty, and I.-O. Stamatescu, Eur.Phys.J. **A49**, 89 (2013), arXiv:1303.6425 [hep-lat].
[5] G. Aarts, PoS **LATTICE2012**, 017 (2012), arXiv:1302.3028 [hep-lat].
[6] A. Schmidt, Y. D. Mercado, and C. Gattringer, PoS **LATTICE2012**, 098 (2012), arXiv:1211.1573 [hep-lat].
[7] Y. D. Mercado, C. Gattringer, and A. Schmidt, Comput.Phys.Commun. **184**, 1535 (2013), arXiv:1211.3436 [hep-lat].
[8] A. Alexandru, M. Faber, I. Horvath, and K.-F. Liu, Phys.Rev. **D72**, 114513 (2005), arXiv:hep-lat/0507020 [hep-lat].
[9] A. Alexandru and U. Wenger, Phys.Rev. **D83**, 034502 (2011), arXiv:1009.2197 [hep-lat].
[10] K. Langfeld, B. Lucini, and A. Rago, Phys.Rev.Lett. **109**, 111601 (2012), arXiv:1204.3243 [hep-lat].
[11] K. Langfeld and J. M. Pawlowski, Phys.Rev. **D88**, 071502 (2013), arXiv:1307.0455 [hep-lat].
[12] N. Bilic, H. Gausterer, and S. Sanielevici, Phys.Rev. **D37**, 3684 (1988).
[13] N. Bilic and K. Demeterfi, Phys.Lett. **B212**, 83 (1988).
[14] L. Ravagli and J. Verbaarschot, Phys.Rev. **D76**, 054506 (2007), arXiv:0704.1111 [hep-th].
[15] G. Aarts and I.-O. Stamatescu, JHEP **0809**, 018 (2008), arXiv:0807.1597 [hep-lat].
[16] J. Bloch, F. Bruckmann, and T. Wettig, JHEP **1310**, 140 (2013), arXiv:1307.1416 [hep-lat].
[17] J. Bloch, F. Bruckmann, and T. Wettig, (2013), arXiv:1310.6645 [hep-lat].
[18] R. De Pietri, A. Feo, E. Seiler, and I.-O. Stamatescu, Phys.Rev. **D76**, 114501 (2007), arXiv:0705.3420 [hep-lat].
[19] M. Fromm, J. Langelage, S. Lottini, M. Neuman, and O. Philipsen, Phys.Rev.Lett. **110**, 122001 (2013), arXiv:1207.3005 [hep-lat].
[20] E. Seiler, D. Sexty, and I.-O. Stamatescu, Phys.Lett. **B723**, 213 (2013), arXiv:1211.3709 [hep-lat].
[21] J. B. Kogut and L. Susskind, Phys.Rev. **D11**, 395 (1975).
[22] T. Banks, L. Susskind, and J. B. Kogut, Phys.Rev. **D13**, 1043 (1976).
[23] T. Banks *et al.* (Cornell-Oxford-Tel Aviv-Yeshiva Collaboration), Phys.Rev. **D15**, 1111 (1977).
[24] L. Susskind, Phys.Rev. **D16**, 3031 (1977).
[25] T. D. . Cohen, Phys.Rev.Lett. **91**, 222001 (2003), arXiv:hep-ph/0307089 [hep-ph].
[26] P. Hasenfratz and F. Karsch, Phys.Lett. **B125**, 308 (1983).
[27] L. G. Molinari, Linear Algebra and its Applications **429**, 2221 (2008).
[28] A. Maas, L. von Smekal, B. Wellegehausen, and A. Wipf, Phys.Rev. **D86**, 111901 (2012), arXiv:1203.5653 [hep-lat].